EUV reflective coherent diffraction imaging system for wafer metrology

Tao Shen, Paolo Ansuinelli, Iacopo Mochi, Young Woo Kang, Jinho Ahn, et al.

Tao Shen, Paolo Ansuinelli, Iacopo Mochi, Young Woo Kang, Jinho Ahn, Yasin Ekinci, "EUV reflective coherent diffraction imaging system for wafer metrology," Proc. SPIE 12618, Optical Measurement Systems for Industrial Inspection XIII, 126180N (15 August 2023); doi: 10.1117/12.2673832

SPIE.

Event: SPIE Optical Metrology, 2023, Munich, Germany

EUV reflective coherent diffraction imaging system for wafer metrology

Tao Shen[1], Paolo Ansuinelli[1], Iacopo Mochi[1], Young Woo Kang[2], Jinho Ahn[2], and Yasin Ekinci[1]

[1]Paul Scherrer Institute, Villigen PSI, Switzerland
[2]Hanyang University, South Korea

ABSTRACT

Nanoscale non-destructive metrology is a key requirement in several steps of the manufacturing process of modern semiconductor devices. In particular, with the introduction of EUV lithography into the high-volume manufacturing, enabling further shrinking of feature sizes, metrology for future technology nodes will become increasingly challenging. Depending on the specific requirements and constraints of the metrology tasks, the choice of the measurement methods is critical, and sometimes limited. Conventional metrology techniques must be constantly adapted to keep up with the device scaling roadmap. To explore new and easily scalable methods for semiconductor wafer metrology, we developed the EUV reflective grazing-incidence nanoscope (REGINE). REGINE is a lensless nanoscope prototype that combines reflectometry, scatterometry and coherent diffraction imaging (CDI) in a single instrument. Being a lensless imaging system, it is compact, cost-effective, and free of lens-induced aberrations. In this work, we will present the REGINE system and the latest results of reflectometry, scatterometry and EUV pellicle transmission experiments.

Keywords: Reflectometry, Scatterometry, EUV pellicle, wafer metrology, EUV

1. INTRODUCTION

Since its adoption in 2019, EUV lithography has played a pivotal role in semiconductor high volume manufacturing and in keeping Moore's law[1] alive. This technology enables the continued reduction in size of semiconductor devices, which are complex and intricate structures consisting of multiple layers, different materials, and features at the nanometer scale. To ensure their quality and reliability, strict quality control measures and precise metrology are important throughout the fabrication process[2,3] As the demand for smaller and more powerful chips continues to grow, the need for highly accurate metrology becomes increasingly important. In particular, metrology must be able to detect defects as small as a few nanometers in the layers with the smallest features. This emphasis on precise and reliable metrology is vital for driving the ongoing advancements in the semiconductor industry.

REGINE[4,5] is a synchrotron-based instrument installed at the XIL-II beamline of the Swiss Light Source. The illumination wavelength of REGINE can be tuned from 6 to 16 nm. The beam is focused onto the sample surface by an ellipsoidal mirror, while the angle of incidence is tunable from 0 to 30 degrees (grazing). The reflected beam is captured by a 2048×2048-pixel CCD (PI-MTE2) with a pixel size of 13.5 µm. The system overview is shown in Figure 1. Most of the components are enclosed in a high vacuum chamber that operates between 10^{-7} and 10^{-8} mbar. REGINE offers two operation modes, reflection and transmission, each with adjustable wavelengths and incidence angles. In reflection mode, the system is used to perform reflectometry, scatterometry[6] and CDI experiments for the characterization of thin films,[7] periodic structures[8] and logic-like/random patterns, respectively. In transmission mode, REGINE enables scatterometry and CDI experiments when the patterns are located on a thin membrane. Additionally, REGINE can be used to measure the transmission of membranes, and in particular EUV pellicles.

Thanks to its short wavelengths, REGINE has a higher resolution compared other tools using visible or UV light. When the system is used for coherent diffraction imaging, its theoretical resolution is 39 nm while using 13.5 nm illumination wavelength.

Further author information: E-mail: tao.shen@psi.ch

Optical Measurement Systems for Industrial Inspection XIII, edited by Peter Lehmann,
Proc. of SPIE Vol. 12618, 126180N · © 2023 SPIE · 0277-786X
doi: 10.1117/12.2673832

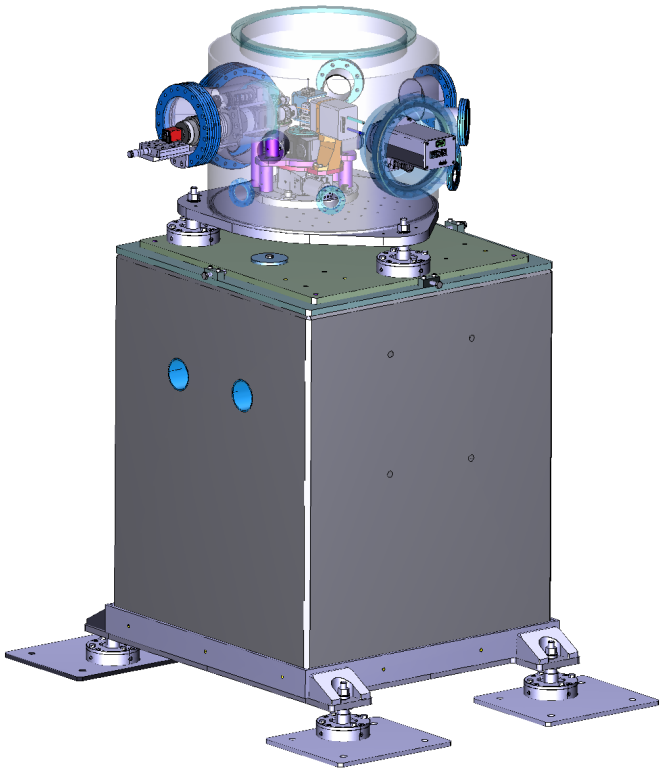

Figure 1: REGINE imaging system. Most of the components are in a high vacuum chamber that usually operates at a pressure between 10^{-7} and 10^{-8} mbar.

To showcase the capabilities of the tool, the experiments we discuss here include reflectometry, scatterometry, and transmission measurements. The measurement of the reflectance or the transmittance of a sample is performed by evaluating the ratio of the reflected or transmitted intensity and the intensity recorded in absence of the sample (reference). Scatterometry measurements are performed through the analysis of the diffraction pattern generated by a scattering sample.[8] Because we make use of the recorded intensity values to calculate the reflectance and the transmittance of our samples, we need to ensure that the data we use is collected in the linear response range of our detector.

As the REGINE illumination system is diffraction limited, when we perform reflectance and transmittance measurements, the intensity distribution captured on the CCD is an Airy pattern given by:

$$I(r) = I_0 \left[\frac{2J_1(r)}{r}\right]^2 \tag{1}$$

Where J_1 is the Bessel function of the first kind and I_0 is the peak intensity. To calculate the reflectance and the transmittance of the samples, we fit the recorded intensity distribution in the detector linear range to an analytical model described in equation 1. This procedure, shown in Figure 2, is applied to both measured data and reference.

2. EXPERIMENTS AND RESULTS

The first experiment we present here is a simple reflectometry test performed on a EUV mask blank, i.e. substrate coated with a Mo-Si multilayer with optimized parameters of maximum EUV reflectance at 6° of incidence angle from the surface normal. The experiment was conducted with 13.5 nm illumination wavelength and five different grazing incidence angles (2.6°, 6.6°, 10.6°, 14.6°, 26.6°). We scanned a 3 mm × 3 mm area near the center

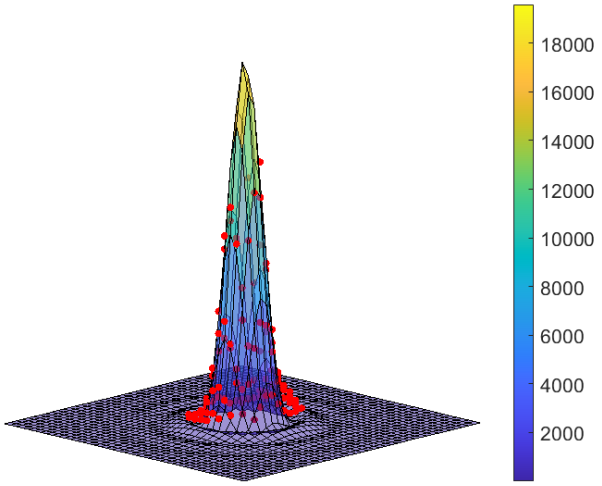

Figure 2: Reflectometry data and its fitting model. Red dots are the data points, and they are fitted with an airy pattern. The maxima of the fitted airy pattern is used for the reflectance calculation.

of the sample. Then, the sample was moved out of the beam path to measure the direct beam as a reference dataset. We repeated this procedure with different incidence angles. A summary result from one of the samples we investigated is shown in Figure 3. For each of the incidence angles, we calculated the average reflectance of all the data points within the scan area, and their standard deviation. We observed that at the grazing incidence angle of 26.6°, the standard deviation of the dataset is much smaller than other angle's datasets. That is because at this large angle, the reflectance is significantly less than other angles, and it is less sensitive to the local property changes of the sample surface. The results we obtained can be used to fit the model of the multilayer of photomask to determine its structural and compositional properties.

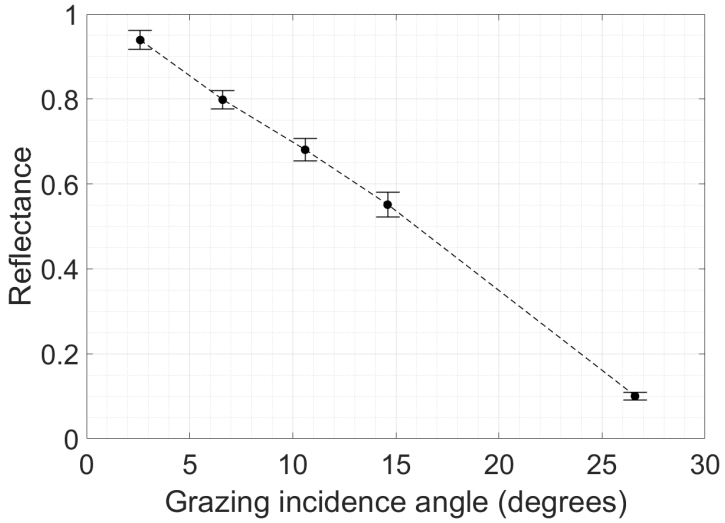

Figure 3: Average reflectance for one of the samples at different incidence angles.

We also performed scatterometry measurements to validate our scatterometry simulation model and data analysis algorithm. A line-space grating was illuminated in conical diffraction mounting, as shown in Figure 4.

Figure 5a shows the diffraction pattern recorded on the CCD. In order to calculate the distances of each order to the zero order, we corrected the conical diffraction effect[9] as shown in Figure 5b. This allowed us to verify that the grating pitch of our sample is 370 nm from the grating equation 2

$$\begin{aligned} m \cdot \lambda &= p \cdot \sin\theta \\ X &= L \cdot \tan\theta \end{aligned} \tag{2}$$

where m is the diffraction order number, λ is the illumination wavelength, p is the grating pitch, θ is the diffraction angle, X is the distance between the zero order and the m order, and L is the distance between the grating and the CCD.

Figure 6a shows the experimental result and the simulation. The simulation intensities are normalized to the first positive order of the experimental data. When we superpose the two plots in Figure 6b, the positions of the diffraction orders position are matching within our resolution, while we observe significant differences in the intensities of some diffraction orders. The mismatch of the intensity indicates that our simulation model needs to be modified, to include more variables such as the sidewall angle of the grating, the surface roughness, and the carbon layer thickness, etc. The further improvement of the simulation model is still ongoing.

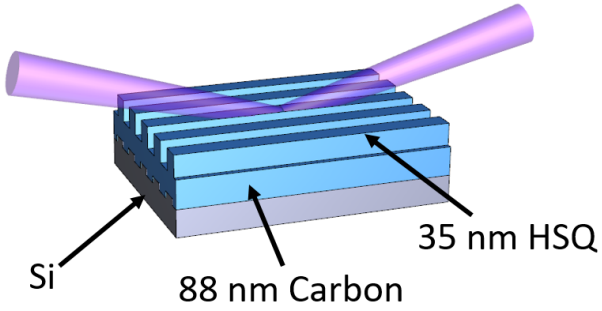

Figure 4: The sample has 35 nm tall HSQ line-space grating on top of a 88 nm carbon layer, on a Si wafer substrate. The grating is designed to have a critical dimension of 200 nm, and a duty cycle of 50%. The sample is in conical diffraction mounting, and the purple parts are the illustration of incident and diffracted beams.

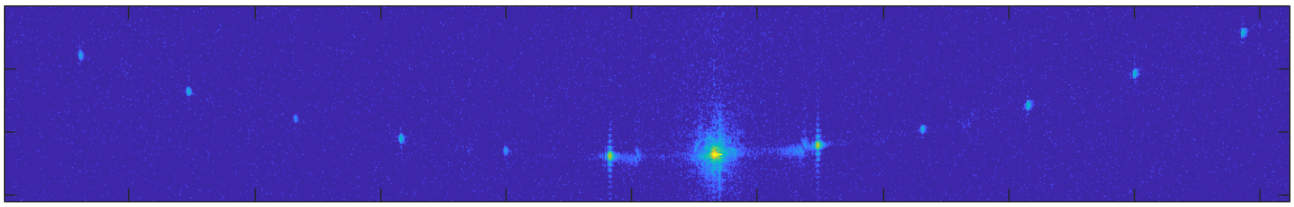

(a) The recorded diffraction pattern

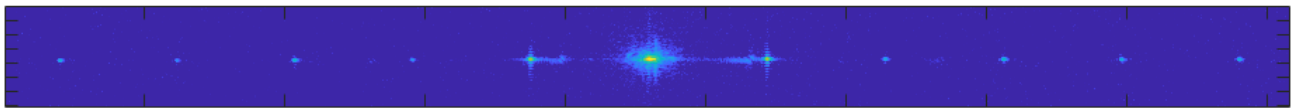

(b) The diffraction pattern after conic effect correction

Figure 5: The original diffraction pattern and after conic effect correction.

Additionally, we measured the transmission of EUV pellicles. The pellicle samples have the size of 1.5 mm ×6 mm. A 5 mm linear scan at the half width position was performed for three different samples, and their transmission data points are plotted in Figure 7. Figure 8 shows the average transmission of the measured positions for each of the samples. All of them are matching the expected transmission value reasonably well.

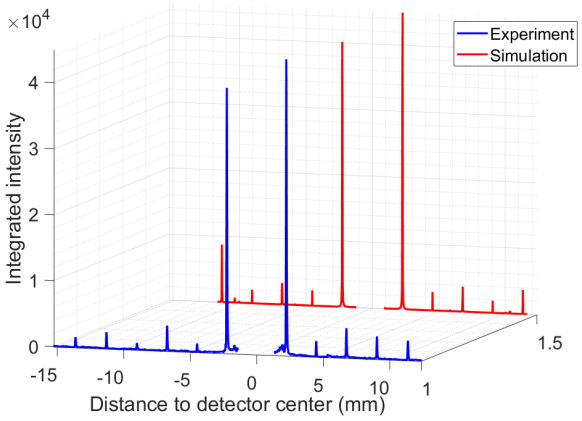

(a) Simulation and experimental diffraction orders

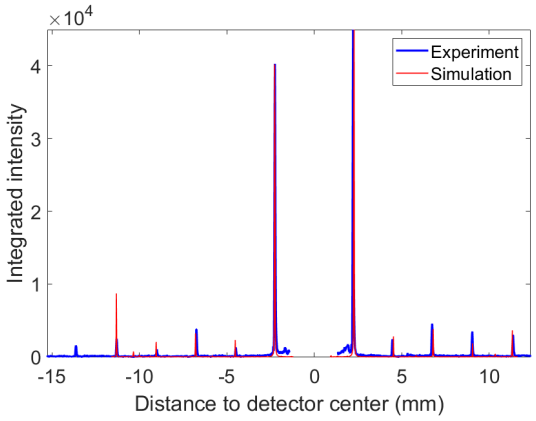

(b) Superposition of the simulation and experimental data

Figure 6: Simulation and experimental data. Zero order is cut away for better visualization purpose.

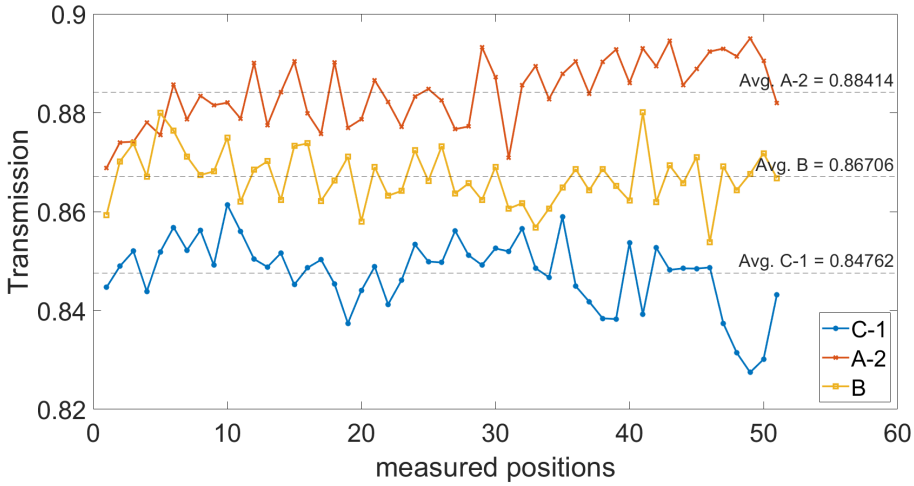

Figure 7: The measured transmission for three EUV pellicles.

3. CONCLUSIONS AND OUTLOOK

The REGINE system is not only designed as a coherent diffraction imaging tool, but also a platform that performs reflectometry, scatterometry, and transmission measurements. It can potentially provide an alternative option for the semiconductor industry to run several metrology measurements with a single tool. At the moment, we successfully implemented reflectometry and transmission measurements, as well as partially validated our scatterometry simulation model and data analysis algorithm. The next steps consist of improving the scatterometry model and completing the development of a grazing incidence CDI algorithm.

ACKNOWLEDGMENTS

The authors thank the XIL-II beamline team of the Swiss Light Source; Markus Kropf, Michaela Vockenhuber, and Istvan Mohacsi, for their technical support, and Dimitrios Kazazis for fabricating the line-space grating sample. We thank our collaborator Dongmin Jeong from Hanyang University for providing the EUV photomask blank samples. The authors also thank the SAMSUNG global research outreach funding for the financial support.

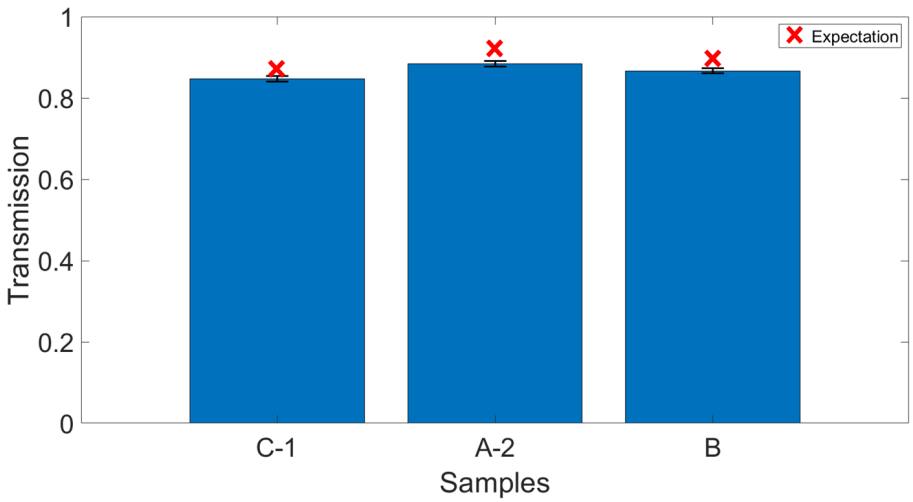

Figure 8: The average transmission of the measured positions and their theoretically estimated transmission. The expected values are based on the expected composition and thickness of the samples, and listed optical constants in literature.

REFERENCES

[1] Moore, G. E., "Gramming more components onto integrated circuits," *Electronics* **38**, 8 (1965).

[2] Diebold, A. C., [*Handbook of silicon semiconductor metrology*], CRC Press (2001).

[3] Orji, N. G., Badaroglu, M., Barnes, B. M., Beitia, C., Bunday, B. D., Celano, U., Kline, R. J., Neisser, M., Obeng, Y., and Vladar, A., "Metrology for the next generation of semiconductor devices," *Nature electronics* **1**(10), 532–547 (2018).

[4] Shen, T., Ekinci, Y., and Mochi, I., "Reflective grazing incidence euv nanoscope for wafer metrology," in [*International Conference on Extreme Ultraviolet Lithography 2022*], **12292**, 194–200, SPIE (2022).

[5] Shen, T., Ansuinelli, P., Mochi, I., and Ekinci, Y., "Euv grazing-incidence lensless imaging wafer metrology," in [*Metrology, Inspection, and Process Control XXXVII*], **12496**, 262–269, SPIE (2023).

[6] Raymond, C., "Overview of scatterometry applications in high volume silicon manufacturing," in [*AIP Conference Proceedings*], **788**(1), 394–402, American Institute of Physics (2005).

[7] Doering, S., Hertlein, F., Bayer, A., and Mann, K., "Euv reflectometry for thickness and density determination of thin film coatings," *Applied Physics A* **107**, 795–800 (2012).

[8] Madsen, M. H. and Hansen, P.-E., "Scatterometry—fast and robust measurements of nano-textured surfaces," *Surface Topography: Metrology and Properties* **4**(2), 023003 (2016).

[9] Gardner, D. F., Zhang, B., Seaberg, M. D., Martin, L. S., Adams, D. E., Salmassi, F., Gullikson, E., Kapteyn, H., and Murnane, M., "High numerical aperture reflection mode coherent diffraction microscopy using off-axis apertured illumination," *Optics express* **20**(17), 19050–19059 (2012).